

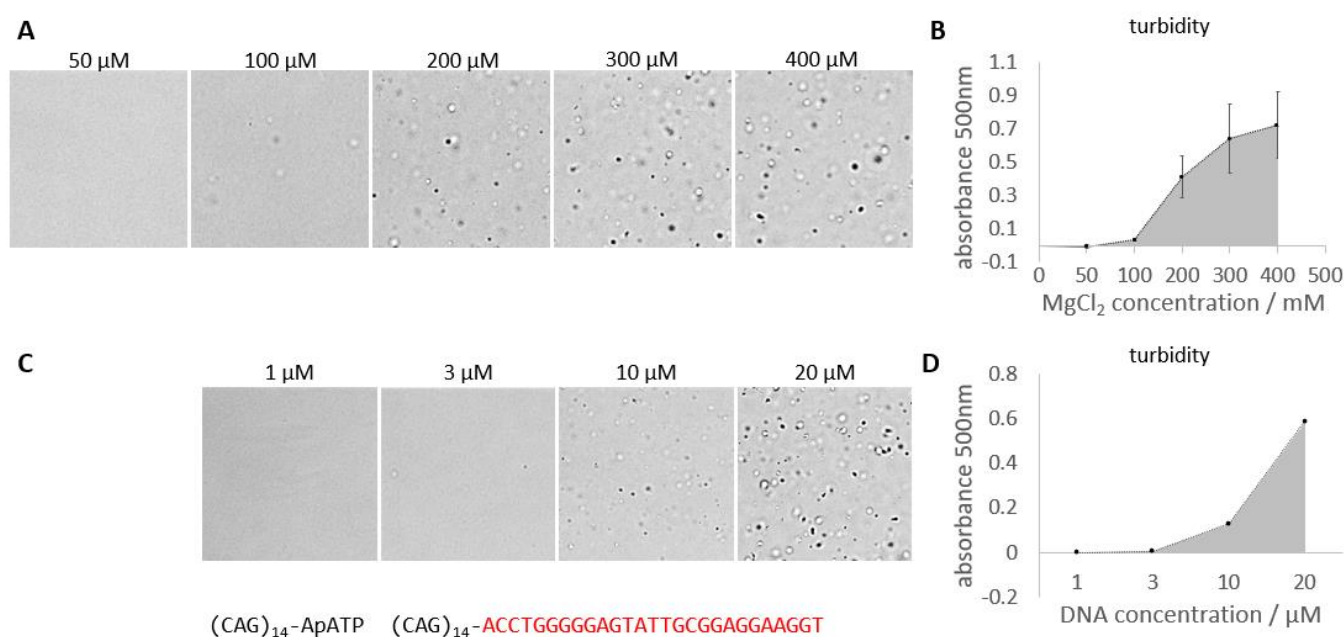
Supplementary Information

# Chemical control of phase separation in DNA solutions

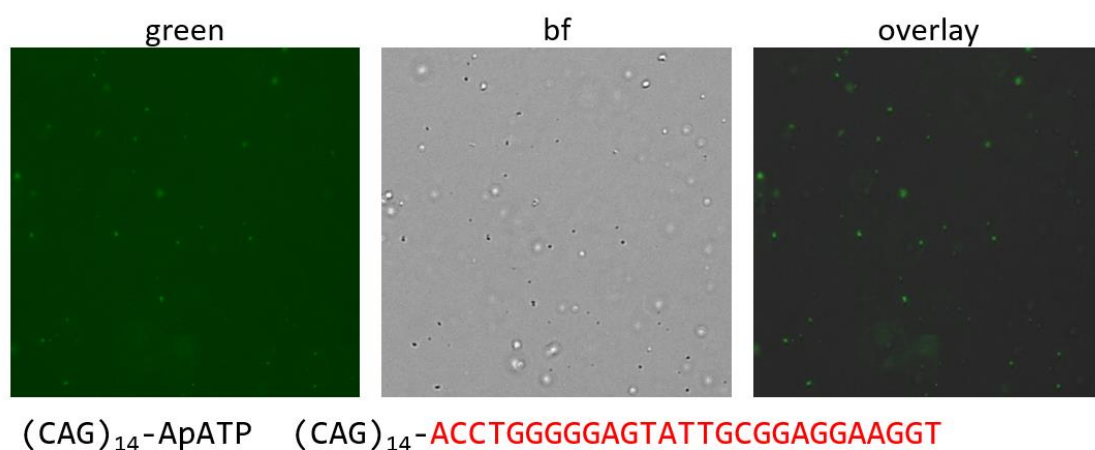
Samuel Hauf<sup>a</sup> and Yohei Yokobayashi\*<sup>a</sup>

<sup>a</sup> Nucleic Acid Chemistry and Engineering Unit  
Onna, Okinawa, Japan 904-0495  
E-mail: yohei.yokobayashi@oist.jp

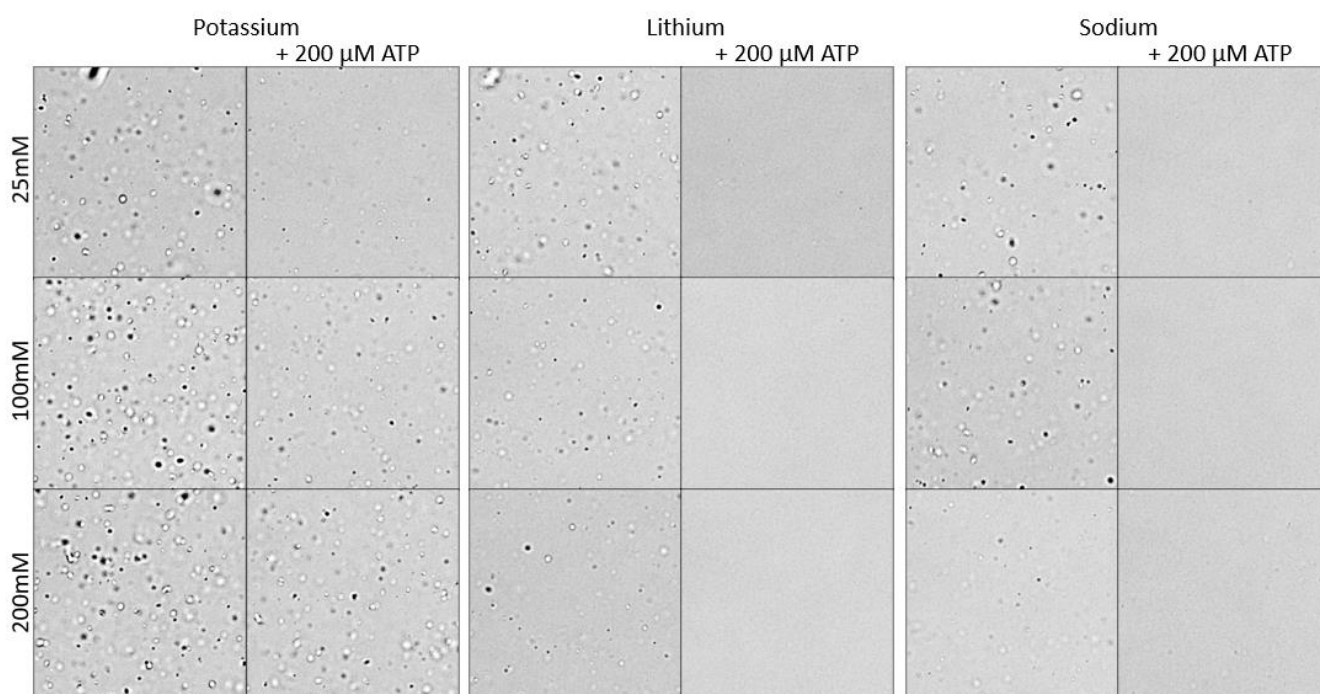
## Supplementary Figures



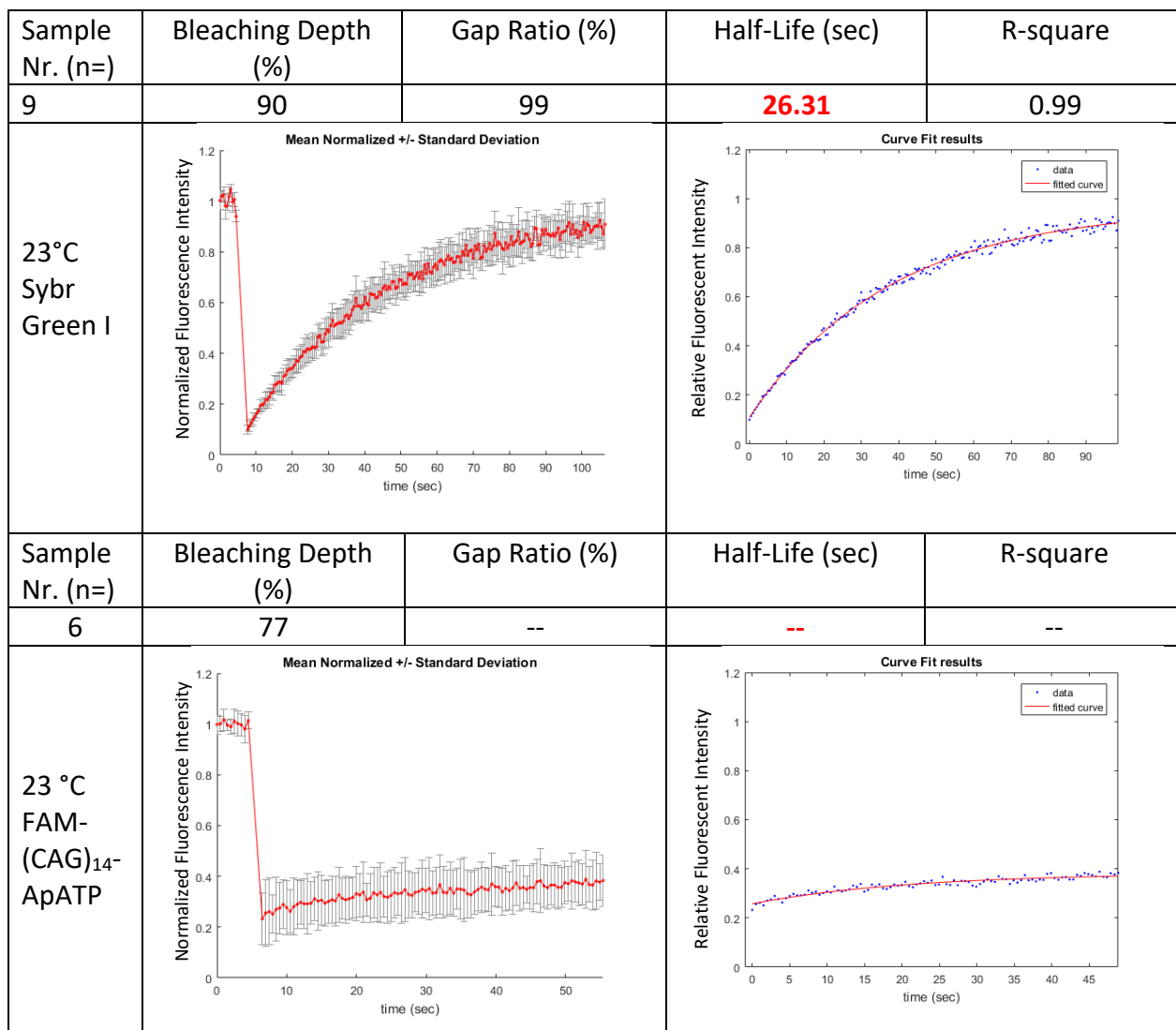
**Figure S1.** Mg<sup>2+</sup> and DNA dependence of phase separation of (CAG)<sub>14</sub>-ApATP. (A) At 20  $\mu\text{M}$ , (CAG)<sub>14</sub>-ApATP only forms visible aggregates at  $\geq 100$  mM MgCl<sub>2</sub> in 10 mM Tris-HCl pH 7.0, 25 mM NaCl. (B) Turbidity measured as absorbance at 500 nm for the same concentrations. The experiment was repeated three times and the average values are shown with the standard deviation. (C) Microscopic pictures and (D) turbidity measurements showing the dependence of phase separation on the DNA concentration. Here, the final mix was used as a blank before aggregation was induced by heating.



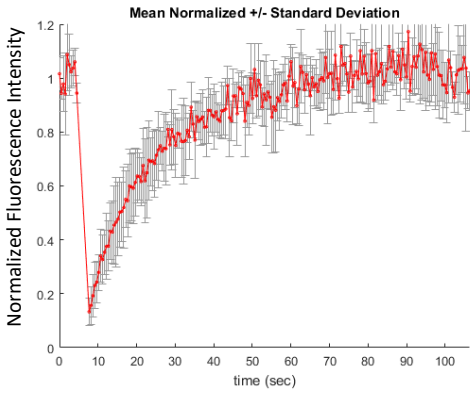
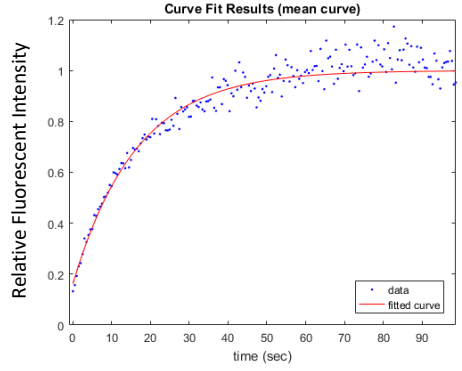
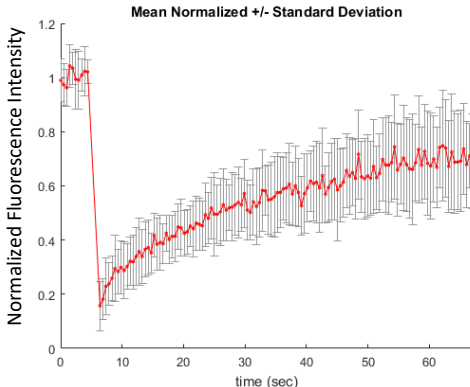
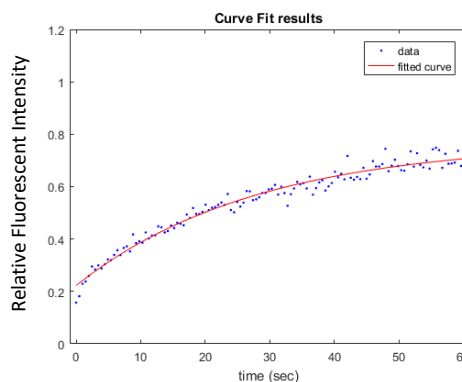
**Figure S2.** (CAG)<sub>14</sub>-ApATP aggregates were stained by 5x SYBR Green I, indicating that they are enriched in DNA. Here, the aggregates were formed as described (20  $\mu$ M oligo DNA, 10 mM Tris-HCl pH 7.0, 25 mM NaCl, 250 mM MgCl<sub>2</sub>) and were stained afterwards by addition of SYBR Green I (10x solution in water) to the final concentration of 5x. The bright field (bf) and the overlay images were adjusted (bf: sharpness +100 %) for better visualization. Note that the aggregates sticking to the surface of the microscopy slide have been imaged and only those aggregates at or close to the focused area show green fluorescence, while more aggregates that are out of focus are still visible in bf. Aggregates out of focus (not sticking to the microscopy slide) were moving rapidly, therefore, they may not overlap properly.



**Figure S3.** Effect of alkali cations (K<sup>+</sup>, Li<sup>+</sup>, and Na<sup>+</sup>) on aggregate stability. K<sup>+</sup> stabilizes the (CAG)<sub>14</sub>-ApATP aggregates (20  $\mu$ M) in 10 mM Tris-HCl pH 7.0 and 250 mM MgCl<sub>2</sub> so that they no longer disappear in the presence of ATP. Aggregates behave similarly in the presence of Li<sup>+</sup> and Na<sup>+</sup>, where the aggregates are less stable at the highest concentration tested (200 mM).



**Figure S4.** FRAP experiments on the (CAG)<sub>14</sub>-ApATP aggregates (20  $\mu$ M) in 10 mM Tris-HCl pH 7.0, 25 mM NaCl, and 250 mM MgCl<sub>2</sub> at room temperature (23 °C). Fast fluorescence recovery of Sybr Green I (2x final concentration) indicates free diffusion of the dye through the aggregates. No significant recovery was observed with the DNA directly labelled with a FAM fluorophore (10 nM). Taken together, these results suggest the aggregates are in a gel-like state at room temperature.

Sample Nr. (n=)	Bleaching Depth (%)	Gap Ratio (%)	Half-Life (sec)	R-square
8	88	99	<b>11.31</b>	0.95
43°C Sybr Green I				
Sample Nr. (n=)	Bleaching Depth (%)	Gap Ratio (%)	Half-Life (sec)	R-square
7	85	90	<b>19.42</b>	0.97
43 °C FAM- DNA				

**Figure S5.** FRAP experiments on the (CAG)<sub>14</sub>-ApATP aggregates (20  $\mu$ M) in 10 mM Tris-HCl pH 7.0, 25 mM NaCl, and 250 mM MgCl<sub>2</sub> at 43°C. Recovery of both Sybr Green I and FAM-DNA fluorescence can be observed indicating that the DNA aggregates are liquid-like at 43°C.

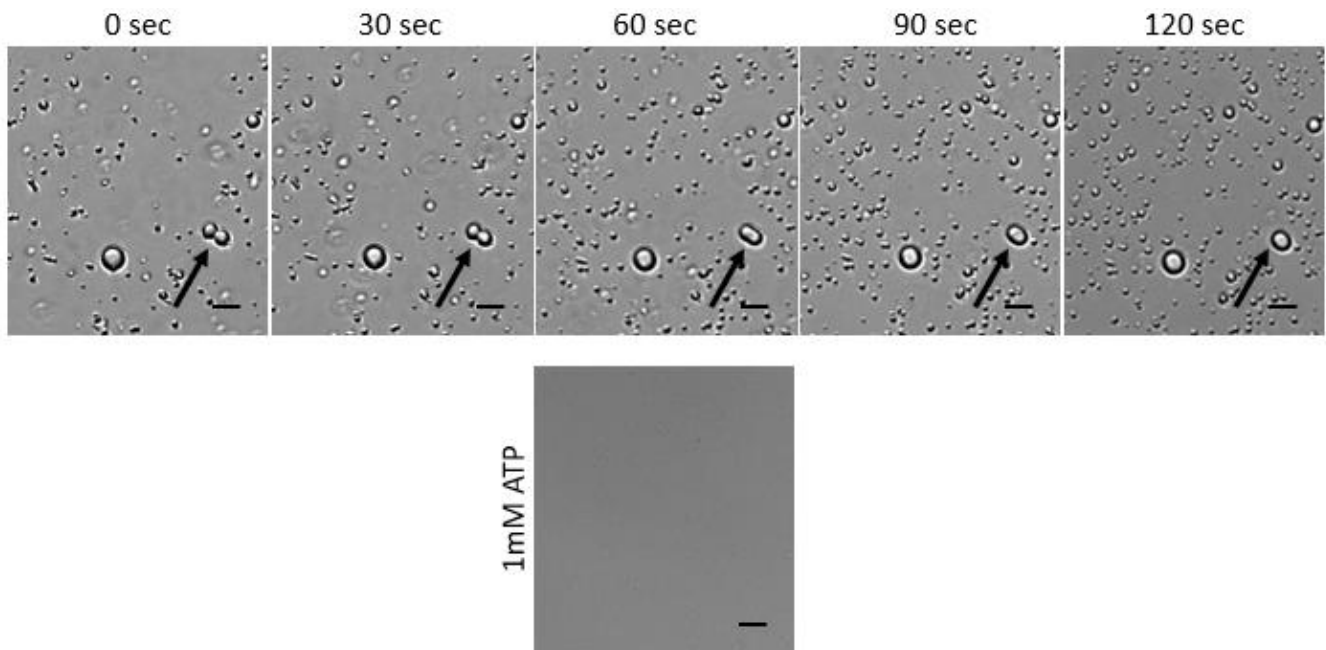


**Figure S6.** Fusion of (CAG)<sub>14</sub>-ApATP (20 μM) droplets could be observed in 10 mM Tris-HCl pH 7.0, 25 mM NaCl, and 250 mM MgCl<sub>2</sub> supplemented with 5 % ethylene glycol at 38°C. In the presence of 1 mM ATP no aggregates were formed. Scale bars indicate 10 μm.

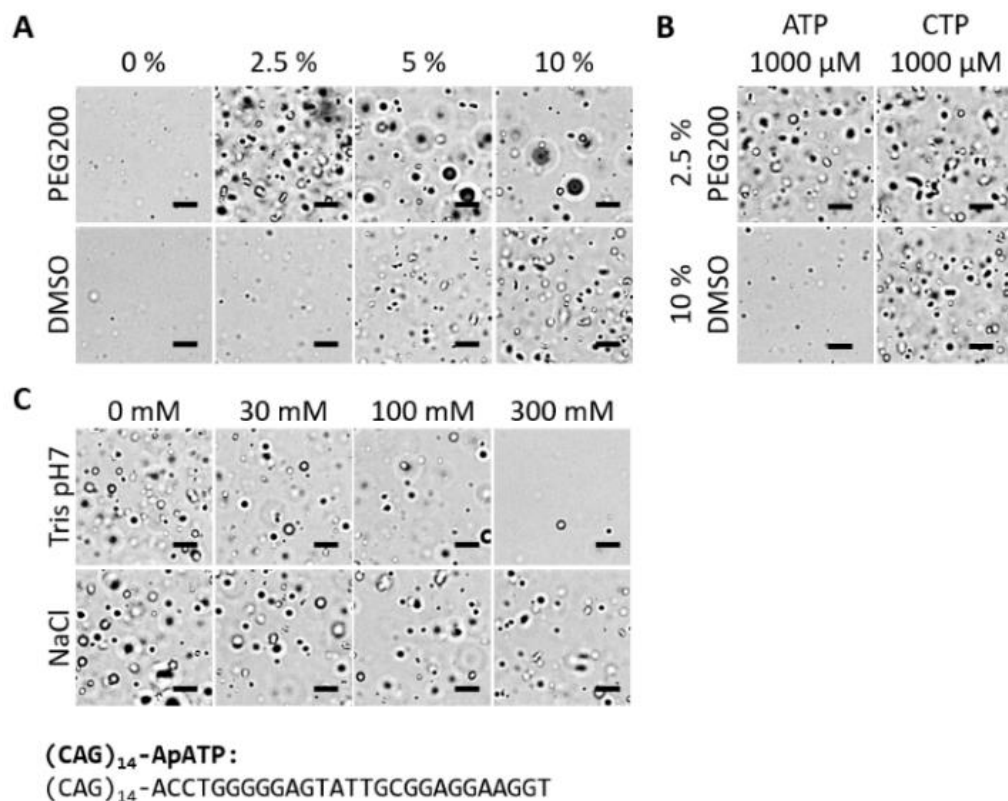


**Figure S7.** Effect of buffer conditions on phase separation of (CAG)<sub>14</sub>-ApATP. (A) Phase separation efficiency could be increased by the addition of DMSO or PEG200 to 10 mM Tris-HCl pH 7.0, 25 mM NaCl, 100 mM MgCl<sub>2</sub>. (B) In the presence of 2.5 % PEG200, the aggregates did not react to ATP, while in 10 % DMSO the aggregates still reacted to the addition of ATP (10 mM Tris-HCl pH 7.0, 25 mM NaCl, 100 mM MgCl<sub>2</sub>). (C) In 100 mM MgCl<sub>2</sub> with 10 % DMSO, NaCl and Tris-HCl concentrations could be varied from 0 to 100 mM without significantly affecting the phase separation. Representative pictures for three independent experiments are shown. Scale bars indicate 10 μm.

For the theophylline DNA aptamer experiments, concentrations were 30  $\mu$ M oligo, 10 mM Tris-HCl pH 7.0, 250 mM  $MgCl_2$ , 25 mM NaCl, and 10 % DMSO. The samples were heated to 46°C for 30 sec before cooling on ice water for 30 sec and immediate imaging.

## Imaging and image processing

For Imaging, 0.5 to 1  $\mu$ l of the solution was spotted on a glass slide (Matsunami Glass) at room temperature, and the aggregates were visualized with an Invitrogen EVOS FL Digital Inverted Fluorescence Microscope (brightfield, 40x objective, 4/10 PH, Diffuser, 72 % intensity). The slide surface was located at the edge of the droplet and the imaging focus adjusted to be shortly above the slide surface inside the solution. Images were then taken near the center of the droplet (away from the edges where evaporation causes movement and accumulation of aggregates). Staining with SYBR Green I was performed after aggregate formation by adding the dye to a final concentration of 5x.

Microscopic images were processed by Microsoft PowerPoint for better visualization of the aggregates. The settings used for all photographs are: sharpness +100 %, contrast +60 %, except if otherwise indicated.

## Quantification from microscopic images

The extent of phase separation was also quantified from the microscopic images by retrieving all pixel intensities (0 – 255) using the ImageJ histogram function. Pixels with intensities between 9 and 245 were then used to estimate the average pixel intensity and the standard deviation to calculate the dispersion index ( $\mu/\sigma^2$ ).

## Quantification by turbidimetry

Phase separation was quantified by measuring the turbidity of the solution (absorbance at 500 nm) at room temperature using the NanoDrop One<sup>C</sup> (Thermo Scientific) with UV-cuvette micro (BRAND). The solutions (80  $\mu$ l) were prepared and heated for 2 min at 95 °C, cooled on ice water for 30 sec, and immediately transferred to cuvettes for absorbance measurement.

## Fusion of droplets

Fusion of droplets could be observed in 10 mM Tris-HCl pH 7.0, 25 mM NaCl, and 250 mM MgCl<sub>2</sub> supplemented with 5 % ethylene glycol at higher temperatures. A cover slide was placed inside a small plastic dish with a tight-fitting lid and water was added on the rim of the dish to generate a water saturated atmosphere and prevent droplet evaporation. Aggregates were generated by thermal cycling as described under “Generation of phase separated aggregates” and a 1.5  $\mu$ l droplet of the solution was placed on top of the cover slide. Then the lid was closed, and the sample was incubated for 2 min at room temperature so that the droplets could settle on the slide surface. The first image was acquired (0 sec). Afterwards, the dish was placed on top of a BioRad T100 Thermal Cycler with the block set to 38 °C and the cover set to 65 °C. The sample was incubated on top of the cycler block for 30 sec before the next image (30 sec) was acquired at room temperature. Other images were acquired after additional incubations (30 sec each) on top of the cycler.

## FRAP

A Nikon A1R laser scanning confocal microscope on a fully motorized inverted microscope (Nikon TiE2) was used for the FRAP measurements. The system includes as detector an A1-DU4-2 4 unit and a Nikon NV multiport as laser launch. The 488 nm laser line has been used for both bleaching and imaging. A high numerical aperture 100x oil objective lens (CFI Apochromat TIRF 60X / NA 1.49) has been used throughout all the measurement. The FRAP analysis were performed using the following measurements:

1. Fluorescence mean intensity from the FRAP ROI (ROI = region of interest)
2. Fluorescence mean intensity from the whole droplet
3. Fluorescence mean intensity of the background

The background intensity was subtracted from all measurements. Then the bleaching depth and gap ratio (remaining fluorescence after the photobleaching pulse in the whole droplet) were calculated. The first one

gives an indication on the efficiency of the bleaching pulse whereas the second one takes in account the effect of the pulse on the whole droplet. The curves have been normalized correcting for differences from the average pre-bleach intensities and the fluorescence at each point as well as variations of the fluorescence in the whole droplet due to the bleaching caused by the laser during the image acquisition. Single term equations were used to fit the experimental data in order to estimate the half-life and the mobile fraction. A non-linear least squares function has been applied for the curve fitting. Sybr Green I dye was added to the buffer to a final concentration of 2x and FAM-labelled DNA was used at a final concentration of 10 nM in a background of unlabelled DNA.

### **Dissolution of aggregates by ligand addition**

Pre-formed aggregates were made with 20  $\mu$ M oligo ((CAG)<sub>14</sub>-ApATP) in 100 mM Tris-HCl pH 7.0, 100 mM MgCl<sub>2</sub>, 100 mM NaCl, and 10 % DMSO as described above. After heating, the solutions were stored on ice until imaging. One  $\mu$ l solution containing aggregates was spotted on a microscopy slide and imaging was started with the focus in the middle of the droplet. Then, one  $\mu$ l of a 10 mM NTP solution was added. Videos were acquired in standard brightfield mode using a Nikon Ti-E with a 40x objective (Plan Apo  $\lambda$ , NA 0.95) and a Nikon DS-Qi2 camera (1608x1608 pixel, exposure time: 50 ms, 10 fps).

### **Visualization of LLPS in cuvettes**

Phase separation of (CAG)<sub>2</sub>-ApATP (20  $\mu$ M) in the presence of 5 mM spermine, 10 mM Tris-HCl pH 7.0 was visualized in BRAND micro cuvettes. For this purpose, 100  $\mu$ l of the solution were prepared as published<sup>1</sup> and imaged in front of a black background with side lighting.

## **References**

1. A. Jain and R. D. Vale, *Nature*, 2017, **546**, 243-247.